

Influence of Ni and Zn substitution on anisotropy of the penetration depth in $\text{La}_{1.85}\text{Sr}_{0.15}\text{CuO}_4$

A. J. Zaleski and J. Klamut

*Institute of Low Temperature and Structure Research, Polish Academy of Sciences, P.O. Box 1410, 50-950 Wroclaw, Poland
and International Laboratory of High Magnetic Fields and Low Temperatures, 95, Gajowicka Street, 53-529 Wroclaw, Poland*

(Received 1 June 1998; revised manuscript received 25 January 1999)

In this paper we present measurements of the penetration depths $\lambda_{ab}(T)$ ($H\parallel c$) and $\lambda_{\perp}(T)$ ($H\perp c$) in $\text{La}_{1.85}\text{Sr}_{0.15}\text{Cu}_{1-x}M_x\text{O}_4$ for $x=0, 0.005, 0.01, 0.015, 0.025,$ and 0.035 for $M=\text{Ni}$ and $x=0, 0.005, 0.01,$ and 0.02 for $M=\text{Zn}$. The penetration depth was obtained from ac susceptibility measurements of powdered samples, immersed in wax, and magnetically oriented in a static magnetic field of 10 T. The temperature dependencies of the penetration depths can be described by power laws, but with exponents n varying linearly with substituent content. The exponent n increases at a rate of about 1 per at. % for nickel substitution and 2.5 per at. % for zinc substitution. We also have found that the penetration-depth anisotropy is dependent on substituent content, decreasing to a minimum at $x\approx 0.015$ and increasing for higher substitutions. The penetration-depth anisotropy vs substituent content can be described by similar quadratic functions for both substituents. Our results strongly suggest that both the effective mass and the density of charge carriers must be taken into account in theories describing high-temperature superconductivity. [S0163-1829(99)08417-9]

I. INTRODUCTION

The most distinctive difference between the low-temperature superconducting materials and the high-temperature superconducting (HTS) cuprates is the magnitude of the anisotropy of superconducting properties in the latter. These cuprates may be considered as stacks of superconducting CuO_2 planes separated by bridging blocks, which act as charge reservoirs for the planes. The different properties of these materials are associated with different strengths of interlayer Josephson coupling. Studies of the low-temperature electromagnetic response may help in understanding the potential mechanisms leading to the occurrence of superconductivity in this system. For d -wave pairing, a spin-fluctuation model may be applicable,¹ whereas the BCS model² is used for conventional low-temperature superconductors with s -wave-type pairing.

The existence or nonexistence of zeros in the superconducting energy gap and their locations on the Fermi surface can be investigated by experimental techniques that are sensitive to low-lying excitations. The temperature (T) dependence of the penetration depth λ (Refs. 3–6) is useful in clarifying the situation, since exponential behavior of $\lambda(T)$ is expected for an isotropic gap, while the presence of the nodes in the gap gives a power-law dependence.

Substitution of copper in superconducting planes with magnetic or nonmagnetic ions provides an additional way of distinguishing between different symmetries of the pairing state. The spin-fluctuation model⁷ predicts that nonmagnetic zinc will be a stronger pair breaker than magnetic nickel when it substitutes for copper in the CuO_2 plane. The different pair-breaking properties of Zn and Ni also should be revealed in London penetration-depth studies.

The magnitude of the penetration-depth anisotropy is influenced not only by the crystal-lattice anisotropy, but also by the dopant concentration and the shape of the Fermi surface. The density of excited quasiparticles [$n_s(0) - n_s(T)$] [where $n_s(T)$ is the density of condensed electrons at tem-

perature T], effective-mass changes, and the density and type of defects may also influence the penetration depth.

We note that the in-plane penetration depth $\lambda_{ab}(T)$ for $H\parallel c$ reflects the properties of the superconducting CuO_2 planes, while the penetration depth $\lambda_{\perp}(T)$ for $H\perp c$ is influenced both by the CuO_2 -plane properties and the Josephson coupling between them.

Many different techniques have been employed to obtain the penetration depth, depending upon whether the superconducting material was in the form of single crystals, thin films, or bulk ceramics. For single-crystalline samples, surface impedance,⁸ microwave inductance,⁹ infrared reflectivity or transmission,¹⁰ magnetic torque,¹¹ and muon-spin relaxation are the main techniques¹² that have been used. For thin films, the mutual-inductance method¹³ has been the primary technique employed, but also infrared¹⁴ and transmission-line techniques¹⁵ have been used. For ceramic or powdered (usually magnetically aligned¹⁶) samples, the penetration depth has been derived from magnetization measurements in both low fields¹⁷ and high fields, where the magnetization is reversible.¹⁸ The penetration depth also has been determined from tunneling,¹⁹ magneto-optical,²⁰ scanning Hall probe,²¹ and electron spin resonance²² measurements.

The most reproducible determinations of the penetration depth seem to have been obtained from positive muon-spin-rotation measurements. This technique yields only the penetration depth λ_{ab} within the superconducting CuO_2 planes, which are common to all high- T_c superconductors. However, since HTS properties also depend upon the quality of the blocking layers and the number of CuO_2 planes in a unit cell, it is important to examine also the penetration depth perpendicular to the CuO_2 planes. This can be done effectively using magnetically aligned superconducting powders.¹⁶

The aim of our investigation was to find out how Cu-site substitution with isovalent magnetic or nonmagnetic ions influences the temperature dependence of the penetration depth in ceramic, magnetically oriented $\text{La}_{1.85}\text{Sr}_{0.15}\text{Cu}_{1-x}M_x\text{O}_4$

($M = \text{Ni}$ or Zn). Although penetration-depth anisotropy in $\text{La}_{2-x}\text{Sr}_x\text{CuO}_4$ with different strontium content has been studied by Shibauchi *et al.*²³ and Locquet *et al.*,²⁴ we are not aware of any previous studies of penetration-depth anisotropy in zinc- and nickel-substituted $\text{La}_{2-x}\text{Sr}_x\text{CuO}_4$ samples.

II. EXPERIMENT

Polycrystalline $\text{La}_{1.85}\text{Sr}_{0.15}\text{Cu}_{1-y}\text{M}_y\text{O}_4$ ($M = \text{Zn}$ or Ni) samples were prepared using the standard solid-state-reaction method, with appropriate amounts of La_2O_3 , SrCO_3 , CuO , ZnO , and NiO taken as starting materials. After two cycles of grinding and calcining at 920 and 945 °C, the powder was ground, pressed into pellets, and fired at 1020 °C (24 h), 1050 °C (24 h), and 1100 °C (48 h). The samples then were annealed at 920 °C (12 h), cooled to 445 °C, annealed at this temperature for 48 h, and slowly cooled to room temperature.²⁵

X-ray data showed that all our samples were single phase with the K_2NiF_4 -type structure. Ceramic samples were re-ground in an agate mill for about 100 min. Powdered samples were magnetically aligned in molten Okerin wax in a static magnetic field of 10 T. The wax was cooled through the melting point while in this field. Small parallelepiped blocks of dimensions $2 \times 2 \times 10 \text{ mm}^3$, with their c axes parallel and perpendicular to the longest dimension, were cut from the composite using a saw. Grain-size distributions were determined from scanning electron microscope (SEM) photographs of different parts of these blocks.

ac measurements were carried out using a commercial Lake Shore ac susceptometer with an amplitude of 0.1 mT and a frequency of 111.1 Hz. From SEM photographs it was seen that the individual grains were well separated. However, since the densities of the wax and powders were different, some sedimentation was unavoidable. We therefore performed additional tests by measuring the linearity of the susceptometer output voltage as a function of the ac-field amplitude and frequency. The output voltage was linear within the limits of $\pm 0.1\%$, indicating that there were no weak links between the individual grains.

The temperature dependence of the penetration depth was determined by a method used earlier by Porch *et al.*²⁶ from the measured ac signal, volume of superconductor, and measured grain-size distribution using the following formulas:

$$\left(\frac{\chi_i}{\chi_0}\right) = \frac{2}{3} \frac{\nu_{ac}}{[V_s N - \nu_{ac}(\frac{1}{3} - D)]},$$

$$\left(\frac{\chi_i}{\chi_0}\right) = \int \left(1 - \frac{3\lambda}{r} \coth \frac{r}{\lambda} + \frac{3\lambda^2}{r^2}\right) r^3 g(r) dr \Big/ \int r^3 g(r) dr,$$

where χ_i is the measured susceptibility in the ab plane or perpendicular to it, χ_0 the susceptibility of a perfectly diamagnetic spherical grain, ν_{ac} the measured ac signal (in μV after subtraction of empty holder signal), V_s the volume of the superconductor (in mm^3), N the calibration factor for ac apparatus (in $\mu\text{V}/\text{mm}^3$ for a perfectly diamagnetic superconductor with $D = 0$), f the volume of a superconductor divided by the total volume of the composite, D the demagnetizing factor of a grain, r the radius of a grain, and $g(r)$ the measured grain-size distribution function.

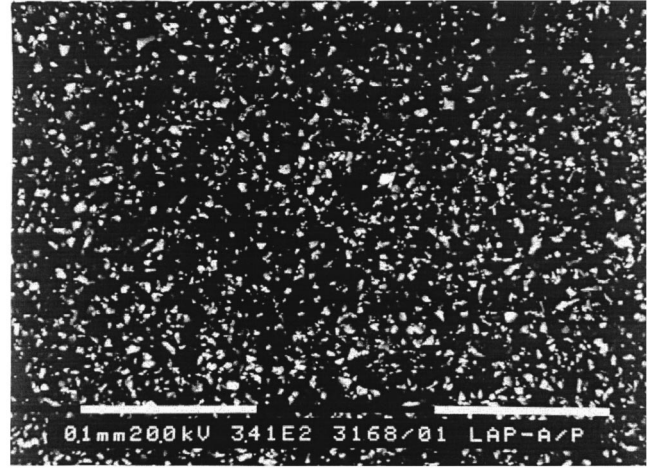


FIG. 1. SEM (scanning electron microscope) photograph of $\text{La}_{1.85}\text{Sr}_{0.15}\text{CuO}_4$ powder in Okerin wax, oriented in a magnetic field. Each white marker is 0.1 mm in length. The magnetic field was oriented perpendicular to the plane of the photograph. The cross-section area of the grains was used for defining their radius.

The above method yields the in-plane penetration depth λ_{ab} when the ac field is oriented perpendicular to the CuO_2 planes, since the induced currents all flow parallel to these planes. We cannot distinguish between the penetration depths λ_a and λ_b for currents along the a and b direction, respectively. When the ac field is oriented parallel to the CuO_2 planes, currents are induced both parallel and perpendicular to the planes, and thus the method yields an effective penetration depth λ_{\perp} , which is a complicated mean value of the in-plane penetration depth λ_{ab} and the out-of-plane c -axis penetration depth λ_c .

If the values of the anisotropic penetration depth are to be obtained from a susceptibility measurement on magnetically aligned powders, first great care has to be taken so that as much as possible of the sample volume consists of properly aligned grains. To achieve this goal, grains of the powder should be single domain. Ball milling rather than grinding was therefore employed. Our powders consisted predominantly of nearly spherically shaped grains. However, grains with different shapes, ranging from short needles to small plates, were also present (an SEM photograph of $\text{La}_{1.85}\text{Sr}_{0.15}\text{CuO}_4$ grains oriented perpendicular to the magnetic field is presented in Fig. 1 as an example). Since a deviation from spherical grain shape influences mainly the magnitude of the penetration depth (our estimated error is below 5%) but has very little effect upon the temperature dependence of λ , we decided to use the demagnetization factor of a sphere for our calculations.

We tested our procedure for penetration-depth evaluation by measuring seven small tin spheres. We chose tin rather than lead, as it was much easier to prevent the tin surface from oxidizing, and therefore diameters of the spheres were more precisely defined. The measured penetration depth extrapolated to zero temperature was 54 nm, which is in excellent agreement with the values obtained by Parr.²⁷

III. RESULTS AND DISCUSSION

The grain distribution was obtained from SEM photographs of different parts of the samples. Histograms obtained

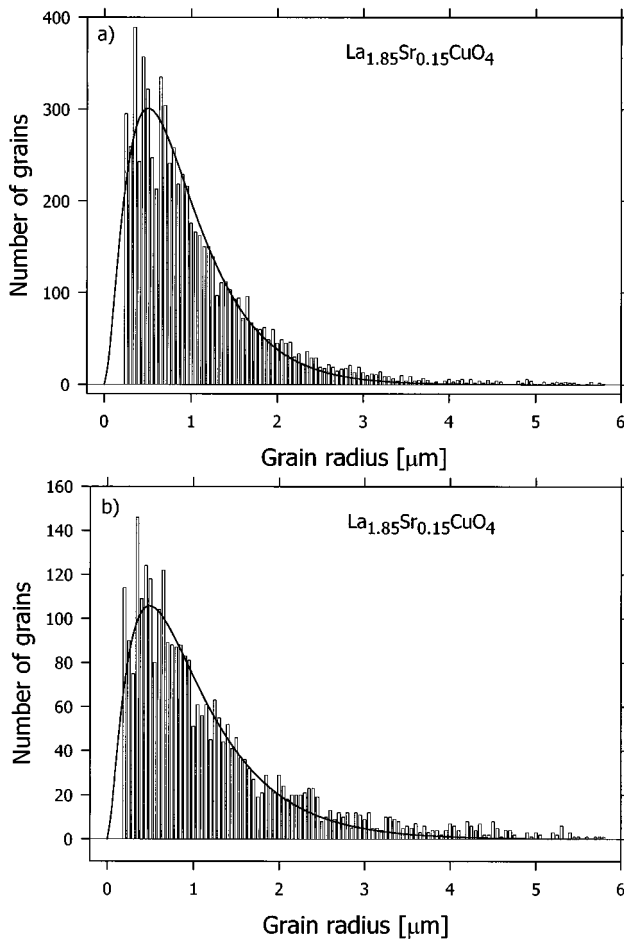


FIG. 2. Histograms of the grain distribution for samples of $\text{La}_{1.85}\text{Sr}_{0.15}\text{CuO}_4$, measured from SEM photographs of sections (a) perpendicular and (b) parallel to the orienting field. Solid curves are fitted to the measured points, and their parameters are taken for penetration-depth evaluation.

from a few of these photographs were fitted to the same function for all samples. Typical histograms for $\text{La}_{1.85}\text{Sr}_{0.15}\text{CuO}_4$ samples cut parallel and perpendicular to the orienting magnetic-field direction are shown in Figs. 2(a) and 2(b) (solid curves show the distribution functions used for the penetration-depth evaluation). The grain diameters varied from 0.2–6 μm with a maximum in the distribution at about 0.6 μm for all samples. Mean radius was derived from the values of the cross sections of the grains seen on SEM photographs, taken perpendicular or parallel to the orienting magnetic field.

The quality of the powder alignment could be estimated from x-ray diffraction patterns. Such patterns are depicted in Figs. 3(a) and 3(b) for Ni- and Zn-substituted $\text{La}_{1.85}\text{Sr}_{0.15}\text{CuO}_4$ samples. As can be seen, almost exclusively 00l reflections are present, their intensity being 30–40 times higher than those for nonoriented samples. Traces of other than 00l reflections arise from the volume of nonaligned material. We have applied the procedure of Ref. 28 to evaluate the percentage of nonaligned grains and found that in all our samples it was within 10–15 %.

Unit-cell parameters were used to calculate the density of superconducting material. These values, together with the results of density measurements of powders immersed in

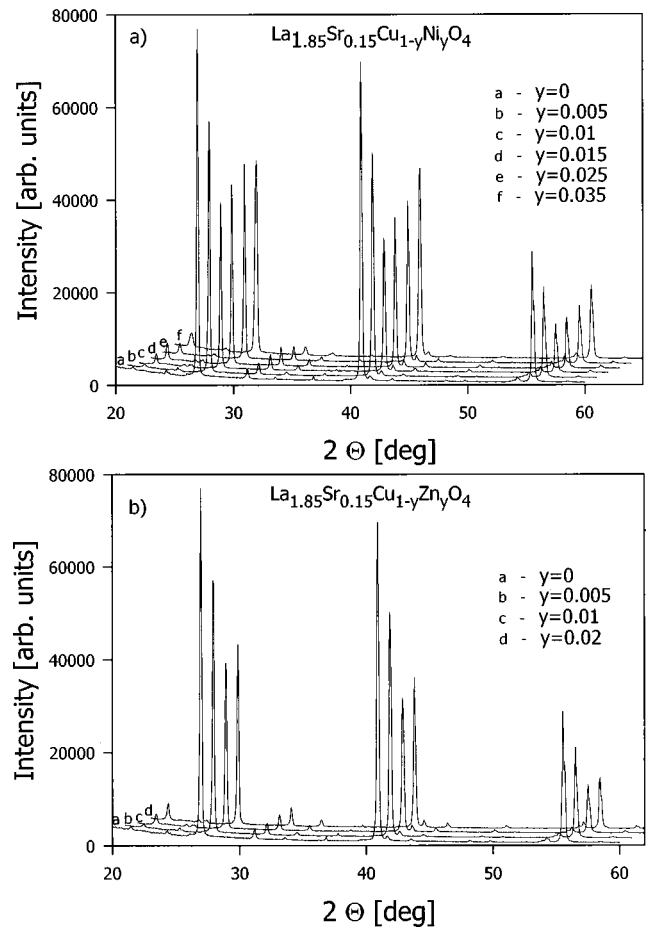


FIG. 3. X-ray diffraction patterns for aligned powders of $\text{La}_{1.85}\text{Sr}_{0.15}\text{Cu}_{1-y}\text{M}_y\text{O}_4$, where (a) $M = \text{Ni}$ and (b) $M = \text{Zn}$ (for clarity, curves are shifted by increments of one degree along the x direction and 1000 arbitrary units along the y direction).

wax, were used to evaluate the volume of superconducting material in the measured samples. The unit-cell parameters for the unsubstituted and the Ni- and Zn-substituted samples are shown in Table I and Fig. 4. The results for the unsubstituted sample are close to the values presented in other papers.^{24,12,29} Although the results for the Ni-substituted samples differ significantly from those presented in Ref. 30, they are similar to those cited by other authors.³¹ Results for the Zn-substituted samples are similar to those published elsewhere.³²

The dependencies of the critical temperature T_c (defined as the onset of the magnetic transition) upon the Zn and Ni concentrations are presented in Fig. 5 and Table I. T_c decreases linearly in both cases but with different slope, namely, -4.1 K/at. % for Ni and -15 K/at. % for Zn.

Similar to the behavior in $\text{YBa}_2\text{Cu}_3\text{O}_{7-\delta}$, the effect of zinc substitution on T_c is about three times stronger than in the case of nickel.³³ This behavior is different from what is observed in conventional superconductors, where magnetic ions such as nickel are strong pair breakers, while nonmagnetic ions such as zinc have a minor effect on T_c . In our view, this clearly supports the idea that substitution by nonmagnetic Zn is nevertheless connected with the induction of a static magnetic moment on the Zn-substituted site.³⁴ A substituted nonmagnetic zinc atom removes a Cu^{2+} spin and

TABLE I. Critical temperature, lattice constants, unit-cell volume, and penetration depth of compounds studied.

Compound	T_c (K)	a, b (nm)	c (nm)	V (nm ³)	$\lambda_{ab}(0)$ (nm)	$\lambda_{\perp}(0)$ (nm)
La _{1.85} Sr _{0.15} CuO ₄	38.9	0.379 49	1.3214	0.190 302	234	547
La _{1.85} Sr _{0.15} Cu _{0.995} Ni _{0.005} O ₄	36.1	0.378 04	1.3227	0.189 033	264	521
La _{1.85} Sr _{0.15} Cu _{0.99} Ni _{0.01} O ₄	33.6	0.378 16	1.3229	0.189 181	351	453
La _{1.85} Sr _{0.15} Cu _{0.985} Ni _{0.015} O ₄	31.7	0.377 58	1.3240	0.188 760	431	436
La _{1.85} Sr _{0.15} Cu _{0.975} Ni _{0.025} O ₄	26.8	0.379 25	1.3218	0.190 110	376	508
La _{1.85} Sr _{0.15} Cu _{0.965} Ni _{0.035} O ₄	23.8	0.378 39	1.3213	0.189 187	210	752
La _{1.85} Sr _{0.15} Cu _{0.995} Zn _{0.005} O ₄	31.9	0.379 83	1.3223	0.190 776	602	932
La _{1.85} Sr _{0.15} Cu _{0.99} Zn _{0.01} O ₄	27.9	0.379 51	1.3219	0.190 384	739	968
La _{1.85} Sr _{0.15} Cu _{0.98} Zn _{0.02} O ₄	17.5	0.378 79	1.3251	0.190 129	664	962

causes its closest Cu neighbors to have partially noncompensated magnetic moments. Nickel, carrying a magnetic moment after substituting copper, introduces only a partial, incremental moment, which may be maximally equal to the difference between Ni and Cu. Thus, substitution of copper by magnetic nickel effectively disturbs the CuO₂ plane less than substitution by nonmagnetic zinc. Thanks to these noncompensated Cu moments around the Zn ion, the area around a zinc impurity also may be excluded from superconductivity, leading to phase separation as in the ‘‘Swiss-cheese’’ model.³⁵ One should bear in mind that since both Zn and Ni have a very similar effect on the normal-state

resistivity, their normal-carrier scattering potential is evidently quite similar.³⁶

The temperature dependence of the normalized penetration depth $\lambda_i(T)/\lambda_i(0)$ for the unsubstituted sample is shown in Fig. 6. It is seen that below about 20 K, this dependence is linear and changes very weakly with temperature (a quadratic dependence has been observed for an underdoped, unsubstituted sample).³⁷

Substitution of copper by nickel or zinc changes the exponent n of the power law describing the low-temperature behavior of the penetration depth $[\lambda_i(T) - \lambda_i(0)]/\lambda_i(0) = AT^n$. This is depicted in Figs. 7(a) and 7(b), where the normalized penetration depths are plotted below 20 K on logarithmic scales for nickel [Fig. 7(a)] and zinc [Fig. 7(b)] substitutions. For nickel, the exponent n changes from one for the unsubstituted sample (Fig. 6) to about four for a Ni concentration of 3.5 at. %. For zinc, these changes are stronger; n varies from one for the unsubstituted sample (Fig. 6) to about five for a Zn concentration of 2 at. %. The exponent n varies nearly linearly with Ni or Zn concentration, with a slope of about 1 per at. % of nickel and about 2.5 per at. % of zinc.

Values of the penetration depths $\lambda_{ab}(0)$ and $\lambda_{\perp}(0)$ for magnetic fields parallel and perpendicular, respectively, to the c axis, extrapolated to zero temperature, are summarized

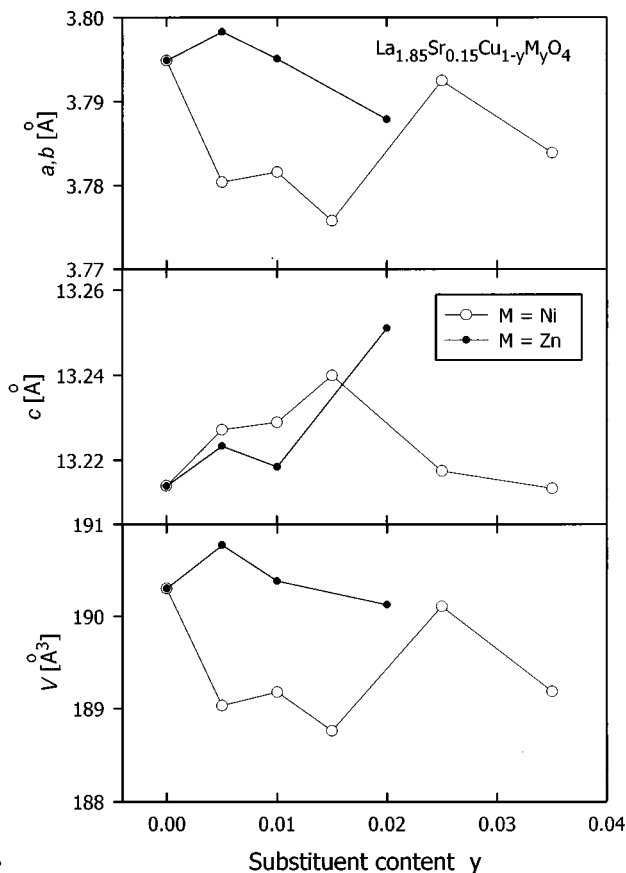


FIG. 4. Nickel- (open circles) and zinc-substituted (closed circles) La_{1.85}Sr_{0.15}CuO₄ unit-cell parameters and volume (lines are merely guides to the eye).

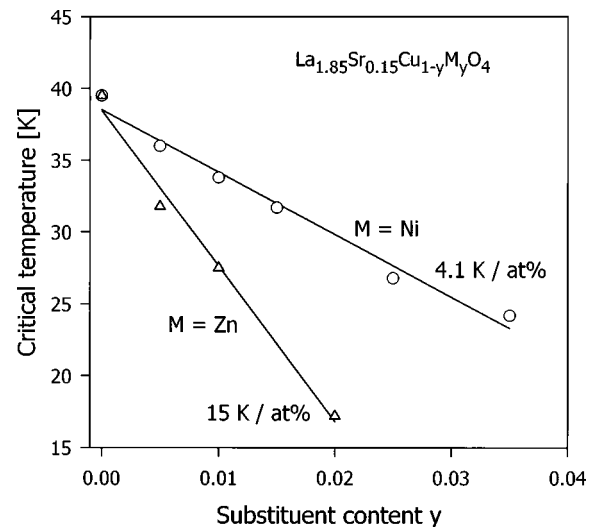


FIG. 5. Critical temperature vs substituent concentration. Solid lines are linear fits to the measured points.

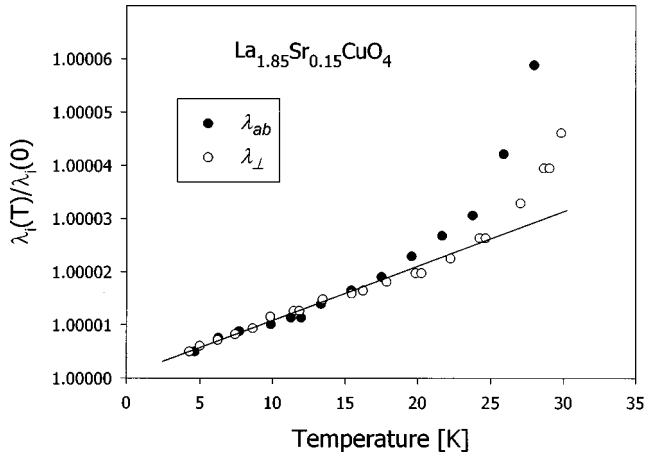


FIG. 6. Temperature dependence of the normalized penetration depth for $\text{La}_{1.85}\text{Sr}_{0.15}\text{CuO}_4$.

in Table I for our samples of $\text{La}_{1.85}\text{Sr}_{0.15}\text{CuO}_4$ substituted with Ni and Zn. The difference between the zinc- and nickel-substitution influence on the superconducting properties of $\text{La}_{1.85}\text{Sr}_{0.15}\text{CuO}_4$ is seen more clearly in Figs. 8(a) and 8(b), where the penetration depths $\lambda_{ab}(0)$ and $\lambda_{\perp}(0)$ for the two substituents are compared.

Substitution first increases the in-plane penetration depth λ_{ab} and then, for concentrations of nickel and zinc above 1.5 at. %, decreases it. The character of changes in λ_{ab} is similar for both substituents, although zinc additions have a much stronger effect upon the penetration depth.

It appears that T_c decreases in substituted $\text{La}_{1.85}\text{Sr}_{0.15}\text{CuO}_4$ because the substituents act as impurities, which shorten the mean free path of the carriers. This mean-free-path shortening leads to an increase of the penetration depth λ_{ab} (but more slowly for nickel than for zinc substitution). From the paper of Nachumi *et al.*³⁵ it is seen that $\text{La}_{1.85}\text{Sr}_{0.15}\text{CuO}_4$ may be treated as overdoped and that increasing the zinc concentration shifts the compound towards the universal $T_c(n_s)$ curve, i.e., towards underdoped region (the ‘‘Swiss-cheese’’ effect³⁵). It also proves that, in spite of the fact that zinc substitution is isovalent, there are still changes of the effective superconducting carrier concentration. It is known³⁸ that in overdoped material, superconductivity can be strongly suppressed by electron-electron scattering, which may be interpreted as a change of the effective mass of the electrons. Zinc doping, shifting the material to the underdoped region, also causes a decrease of electron interaction, reduction of the effective mass, and some decrease of the in-plane penetration depth.

The in-plane penetration depth behavior for nickel has qualitatively similar character to the behavior for zinc. However, since the ‘‘Swiss-cheese’’ scenario is not applicable for nickel, the behavior of λ_{ab} should be connected first of all with the impurity influence. The subsequent decrease of λ_{ab} can be explained by the decoupling of CuO_2 planes.

The main qualitative difference between the influence of both substituents on superconductivity in $\text{La}_{1.85}\text{Sr}_{0.15}\text{CuO}_4$ is seen in the behavior of the effective penetration depth λ_{\perp} ($H \perp c$) [Fig. 8(b)]. Substitution of zinc increases λ_{\perp} very strongly, even for low doping levels. In contrast, nickel substitution first decreases λ_{\perp} and, above 1.5 at. % of Ni, increases it.

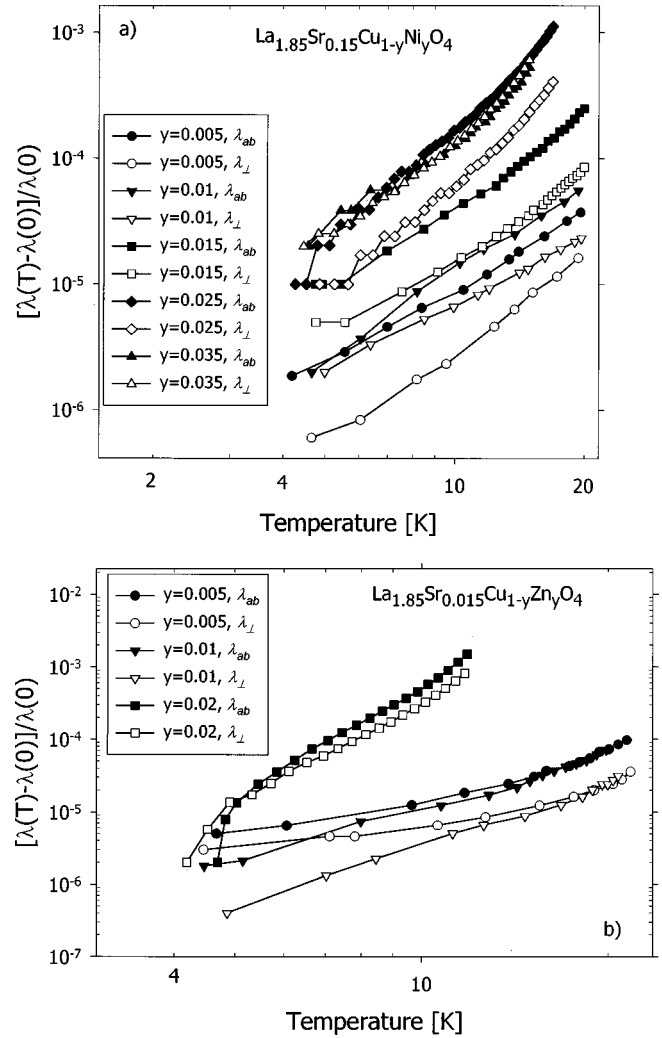


FIG. 7. Double logarithmic plots showing the normalized penetration depths λ_{ab} and λ_{\perp} vs temperature for $\text{La}_{1.85}\text{Sr}_{0.15}\text{Cu}_{1-\gamma}\text{M}_\gamma\text{O}_4$ for substitutions (a) $M=\text{Ni}$ and (b) $M=\text{Zn}$.

The behavior of zinc-doped $\text{La}_{1.85}\text{Sr}_{0.15}\text{CuO}_4$ is easily understood. Normal microregions created in the vicinity of substituents decrease the coupling between the CuO_2 planes, increase the out-of-plane penetration depth λ_c , and hence increase the effective penetration depth λ_{\perp} .

As mentioned earlier, nickel influences the superconducting properties of $\text{La}_{1.85}\text{Sr}_{0.15}\text{CuO}_4$ by acting as a simple impurity scatterer. It has been shown³⁹ that, for tetragonal non-chain superconductors with a gap order parameter of $d_{x^2-y^2}$ symmetry, the c -axis hopping integral is a function of the in-plane momentum. This hopping integral is vanishingly small along the c axis in the vicinity of gap nodes in clean systems. In the case of induced disorder, if the impurity scattering is anisotropic impurity-assisted hopping⁴⁰ might be more important than coherent hopping, and a new conduction channel can be opened, which has a direct contribution to the c -axis superfluid density.³⁹ In our opinion, this mechanism can explain the observed initial decrease of λ_{\perp} for nickel-substituted $\text{La}_{1.85}\text{Sr}_{0.15}\text{CuO}_4$.

It was also stated in Ref. 39 that in the case of a superconductor with d -wave order-parameter symmetry, the disorder connected with substitution has opposite effects on the

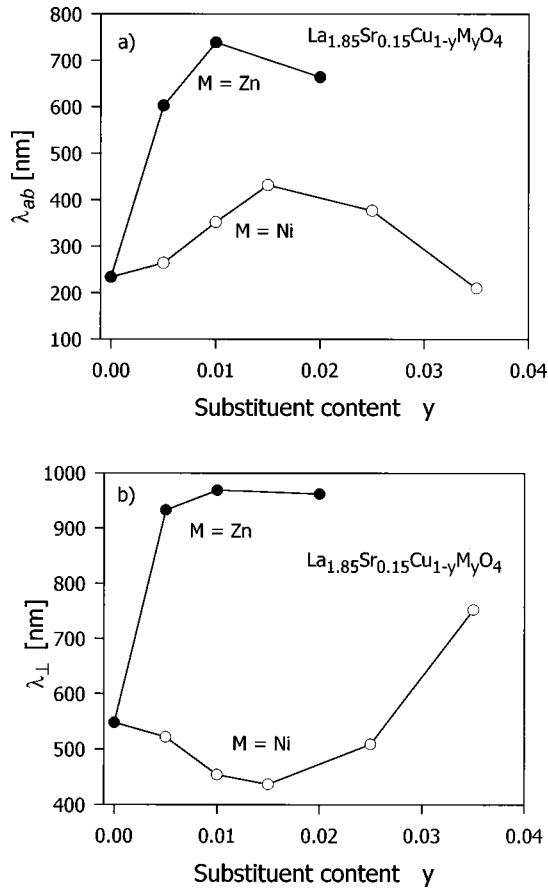


FIG. 8. Penetration depth, extrapolated to zero temperature, vs substituent content for Zn- and Ni-substituted $\text{La}_{1.85}\text{Sr}_{0.15}\text{CuO}_4$: (a) in-plane penetration depth λ_{ab} ($H \parallel c$) and (b) effective penetration depth λ_{\perp} ($H \perp c$).

superfluid response in the ab plane and along the c axis. Thus, changing the impurity concentration should have opposite effects upon the in-plane penetration depth λ_{ab} and the out-of-plane penetration depth λ_c (and hence λ_{\perp}). This is just what is observed for nickel substitution. The initial increase of λ_{ab} with Ni addition evidently is connected with the decrease of λ_{\perp} ; and for large Ni content, the decrease of λ_{ab} is accompanied by an increase of λ_{\perp} .

The influence of zinc on the penetration depth is apparently not limited to the scattering of quasiparticles by impurities as it probably is in the case of nickel. One of the possible effects may be the ability of Zn to alter local spin fluctuations within CuO_2 planes.⁴¹ This would support the view¹ that spin fluctuations are fundamental to high-temperature superconductivity. It seems that the ‘‘Swiss-cheese’’ model can be equally applicable for an explanation of the above-mentioned effect.³⁵

It is interesting to compare the changes of the penetration-depth anisotropy produced by Ni and Zn substituents. These are plotted in Fig. 9 as $(\lambda_{\perp} - \lambda_{ab})/\lambda_{ab}$ vs Ni or Zn concentration. Quadratic fits to the measured points are presented for Ni (dashed curve) and Zn (solid curve). What is surprising is that both fitting curves are almost the same within experimental error. The penetration-depth anisotropy first decreases, almost vanishes for about 1.5% of substitution, and then increases. The magnitude of the penetration depth in zinc-substituted samples is almost twice as high as in nickel-

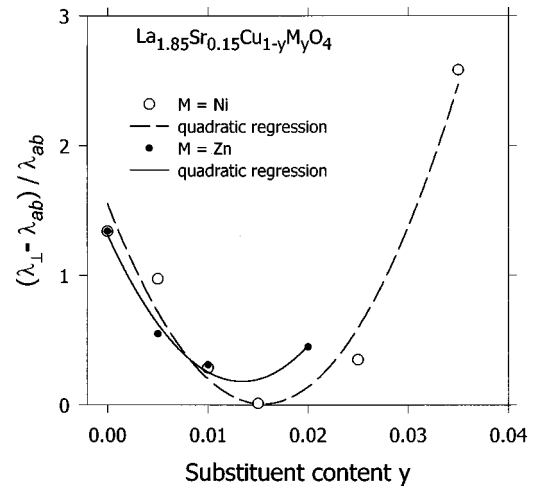


FIG. 9. Penetration-depth anisotropy, $(\lambda_{\perp} - \lambda_{ab})/\lambda_{ab}$ (see Fig. 8), vs substituent concentration in Ni- and Zn-substituted $\text{La}_{1.85}\text{Sr}_{0.15}\text{CuO}_4$. Dashed curve, quadratic fit to measured points (open circles) for nickel substitutions; solid curve, quadratic fit to measured points (closed circles) for Zn substitutions.

substituted ones. The morphology of both sets of samples is the same, and the mean grain radius is also similar. It appears that both impurities change the anisotropy of the penetration depth almost identically, independent of their magnetic properties. This is a surprising fact, especially if one compares the very different behaviors of λ_{\perp} shown in Fig. 8.

The existence of a minimum in the penetration-depth anisotropy vs temperature can be inferred from theoretical papers dealing with c -axis properties of cuprates.^{39,40} It may appear in high- T_c materials, in which the order parameter possesses either s -wave or d -wave symmetry. For s -wave-type materials, the minimum should be rather flat and appear above $0.5T_c$, whereas for superconductors with order parameters of d -wave symmetry, the minimum should be more pronounced, appearing below $0.5T_c$. Thus, the existence of the minimum of anisotropy on substituent content is not surprising. What is unexpected is the fact that, for substituents whose influence on superconductivity is so very different, the minimum in the penetration-depth anisotropy occurs at the same concentration in $\text{La}_{1.85}\text{Sr}_{0.15}\text{Cu}_{0.985}\text{M}_{0.015}\text{O}_4$.

Our investigations indicate that substitutions in $\text{La}_{1.85}\text{Sr}_{0.15}\text{CuO}_4$ first make the material more magnetically isotropic and then strongly decouple the CuO_2 planes. Such a scenario is independent of the physical mechanisms underlying changes of the penetration depth.

In the weak-coupling limit, the square of the penetration depth is proportional to the effective mass of the superconducting carriers and inversely proportional to their density,³⁵

$$\lambda_{\parallel}^2 = c^2 m^* / 4\pi n_s e^2 (1 + \xi/l),$$

where n_s is the concentration of superconducting carriers and m^* is the effective mass, ξ is the coherence length, and l is the mean free path.

Usually changes of the penetration depth are connected with changes in the density of superconducting charge carriers. In our opinion, to explain the substitutional dependence

of the penetration depth, it is necessary to include also the changes of the effective mass of the charge carriers, which reflects the interactions among them. This is particularly important if the substitutions change the material from being underdoped to overdoped. Such a change may occur even if the substitution is isovalent. Substitution with zinc or nickel introduces scattering centers, decreasing the mean free path of the charge carriers and changing the Josephson coupling between the CuO_2 planes. The penetration depth is inversely proportional to both the mean free path and critical Josephson current density,¹⁰

$$\lambda_{\perp}^2 = \hbar c^2 / 8\pi d e J_c,$$

where d is the distance between the planes and J_c is the density of Josephson current between the planes.

Nickel substitutions, acting as simple impurity scatterers, shorten the mean free path of charge carriers within the CuO_2 planes and at the same time open new channels for incoherent current transfer perpendicular to the planes, thereby increasing the Josephson current density in this direction and decreasing the out-of-plane penetration depth λ_c .

It is also seen that the penetration-depth anisotropy of zinc- and nickel-substituted $\text{La}_{1.85}\text{Sr}_{0.15}\text{CuO}_4$ is not connected with the value of the critical temperature. Since we have used isovalent substitutions of copper, the density of charge carriers should be the same for all samples studied. However, the density of carriers taking part in superconductivity may vary if the mean free path is changed by impurities or if strong magnetic (or other) pair breaking exists.

We should also note that the measured penetration-depth anisotropy is much lower than that evaluated from surface impedance measurements for $\text{La}_{1.85}\text{Sr}_{0.15}\text{CuO}_4$.²³ This may be caused by the fact that whereas λ_{ab} ($H\parallel c$) is an intrinsic penetration depth, the effective penetration depth λ_{\perp} ($H\perp c$) is a complicated average of the in-plane penetration depth λ_{ab} and the out-of-plane penetration depth λ_c , which is dominated by Josephson coupling. On the other hand, it is worth mentioning that the values of our penetration depths are similar to those reported in the literature.^{24,12,29}

IV. SUMMARY

In summary, we have used ac susceptibility measurements to determine the influence of isovalent substitution of Zn and Ni for Cu upon the penetration depth in magnetically oriented, ceramic powders of $\text{La}_{1.85}\text{Sr}_{0.15}\text{CuO}_4$ for a broader range of concentrations than has been reported in the literature.

Similar to the behavior in $\text{YBa}_2\text{Cu}_3\text{O}_7$, substitution of Zn for Cu in $\text{La}_{1.85}\text{Sr}_{0.15}\text{CuO}_4$ reduces the critical temperature more strongly (by a factor of about 3) than does substitution of Ni. Such behavior may be explained in the framework of the ‘‘Swiss-cheese’’ model³⁵ in the case of zinc substitution and simple impurity scattering in the case of nickel.

The temperature dependence of the penetration depth is linear for low temperatures in unsubstituted material. For nickel- and zinc-substituted $\text{La}_{1.85}\text{Sr}_{0.15}\text{CuO}_4$, however, the

temperature dependence is still described by a power law (T^n), but with an exponent n different from unity. The dependence of n upon the substituent concentration is stronger for zinc than for nickel, by more than a factor of 2.

The in-plane penetration depth λ_{ab} ($H\parallel c$), extrapolated to zero temperature, has a similar concentration dependence for both Ni and Zn, although the underlying physics of this behavior may be quite different. A qualitative difference was found for the influence of Ni and Zn on the effective penetration depth λ_{\perp} ($H\perp c$). The behavior of the nickel-substituted samples can be explained by the influence of impurity scattering. To account for the influence of zinc on the penetration depth, however, the idea of an effective-mass change in underdoped and overdoped compounds has to be employed.

We have found that nearly the same quadratic law describes the penetration-depth anisotropy vs substituent concentration for both Zn and Ni. From our study, it appears that magnetic nickel acts simply as an impurity, decreasing the mean free path of carriers within the CuO_2 planes and increasing impurity-assisted hopping between the planes.³⁹ Our results support the ‘‘Swiss-cheese’’ model,³⁵ in which some area around each Zn impurity is excluded from superconductivity. This might be connected with the ability of zinc atoms to effectively suppress spin fluctuations.⁴¹ To explain the properties of zinc- and nickel-substituted $\text{La}_{1.85}\text{Sr}_{0.15}\text{CuO}_4$, we found it necessary to treat this superconductor as having d -wave pairing.

Our observation of a minimum in the penetration-depth anisotropy vs substituent content suggests that a complete theory of high-temperature superconductivity must account not only for the impurity concentration and the kinds of impurities but also for the anisotropy of the effective mass of the carriers. Since different physical mechanisms have different influences on the effective-mass components (m_{ab} parallel and m_c perpendicular to the CuO_2 planes), they lead not only to different temperature dependencies predicted in Ref. 40 but also to different dependencies on the impurity concentration. This evidently is the reason for a minimum of the penetration-depth anisotropy vs temperature⁴⁰ and vs impurity concentration (we found this to occur for $x_{\min} \approx 1.5\%$). According to our measurements, the effective masses m_{ab} and m_c have different impurity concentration dependencies. We believe that taking into account changes of both the effective mass and the density of excitations will permit a more effective interpretation of the phenomena connected with high-temperature superconductivity.

Our results also show that coupling between the CuO_2 planes plays an important role in the high-temperature superconductors.

ACKNOWLEDGMENTS

The authors express their gratitude to Tomasz Zaleski for providing computer programs for the SEM photograph analysis and penetration-depth evaluation. We thank Professor John R. Clem for suggestions and help with editing this paper. This work was sponsored under Grant KBN No. 2PO3B15309 and No. 2PO3B05411 (partially).

- ¹P. Monthoux and D. Pines, Phys. Rev. B **47**, 6069 (1993).
- ²J. Bardeen, L. N. Cooper, and J. R. Schrieffer, Phys. Rev. **106**, 108 (1957).
- ³W. N. Hardy, D. A. Bonn, D. C. Morgan, R. Liang, and K. Zhang, Phys. Rev. Lett. **70**, 3999 (1993).
- ⁴N. Klein, N. Tellmann, H. Schultz, K. Urban, S. A. Wolf, and V. Z. Kresin, Phys. Rev. Lett. **71**, 3355 (1993).
- ⁵Z. Ma, R. C. Taber, L. W. Lombardo, A. Kapitulnik, M. R. Beasley, P. Merchant, C. B. Eom, S. Y. Hou, and J. M. Phillips, Phys. Rev. Lett. **71**, 781 (1993).
- ⁶S. M. Anlage, B. W. Langley, G. Deutscher, J. Halbritter, and M. R. Beasley, Phys. Rev. B **44**, 9764 (1991).
- ⁷D. Pines, in *Strongly Correlated Electronic Materials: Los Alamos Symposium 1993*, edited by K. Bedell, Z. Wang, D. E. Meltzer, A. Valatzky, and E. Abrahams (Addison-Wesley, Reading, MA, 1994).
- ⁸A. Maeda, T. Shibauchi, N. Kondo, K. Uchinokura, and M. Kobayashi, Phys. Rev. B **46**, 14 234 (1992).
- ⁹K. Zhang, D. A. Bonn, S. Kamal, R. Liang, D. J. Baar, W. N. Hardy, D. Basov, and T. Timusk, Phys. Rev. Lett. **73**, 2484 (1994).
- ¹⁰D. N. Basov, T. Timusk, B. Dabrowski, and J. D. Jorgensen, Phys. Rev. B **50**, 3511 (1994).
- ¹¹B. Janossy, D. Prost, S. Pekker, and L. Fruchter, Physica C **181**, 51 (1991).
- ¹²W. J. Kossler, J. R. Kempton, X. H. Yu, H. E. Schone, Y. J. Uemura, A. R. Moodenbaugh, M. Suenaga, and C. E. Stronach, Phys. Rev. B **35**, 7133 (1987).
- ¹³A. T. Fiory, A. F. Hebard, P. M. Mankevich, and R. E. Howard, Appl. Phys. Lett. **52**, 2165 (1988).
- ¹⁴L. A. de Vaulchier, J. P. Vieren, A. El Azrak, Y. Guldner, N. Bontemps, M. Guilloux-Viry, C. LePaven-Thivet, and A. Perrin, Phys. Rev. B **52**, 564 (1995).
- ¹⁵J. M. Pond, K. R. Carrol, J. S. Horwitz, D. B. Chrisey, M. S. Osovsky, and V. C. Cestone, Appl. Phys. Lett. **59**, 3033 (1991).
- ¹⁶D. E. Farrell, B. S. Chandrasekhar, M. R. DeGuire, M. M. Fang, V. G. Kogan, J. R. Clem, and D. K. Finnemore, Phys. Rev. B **36**, 4025 (1987).
- ¹⁷J. R. Cooper, C. T. Chu, L. W. Zhou, B. Dunn, and G. Gruner, Phys. Rev. B **37**, 638 (1988).
- ¹⁸J. Sok, M. Xu, W. Chen, B. J. Suh, J. Gohng, D. K. Finnemore, M. J. Kramer, L. A. Schwartzkopf, and B. Dabrowski, Phys. Rev. B **51**, 6035 (1995).
- ¹⁹A. G. Sun, D. A. Gajewski, M. B. Maple, and R. C. Dynes, Phys. Rev. Lett. **72**, 2267 (1994).
- ²⁰N. Moser, M. R. Koblischka, H. Kronmuller, B. Gegenheimer, and H. Theuss, Physica C **159**, 117 (1989).
- ²¹A. Oral, S. J. Bending, R. G. Humphreys, and M. Heinini, Supercond. Sci. Technol. **10**, 17 (1997).
- ²²M. Puri and L. Kevan, Physica C **197**, 53 (1992).
- ²³T. Shibauchi, H. Kitano, K. Uchinokura, A. Maeda, T. Kimura, and K. Kishio, Phys. Rev. Lett. **72**, 2263 (1994).
- ²⁴J.-P. Locquet, Y. Jaccard, A. Cretton, E. J. Williams, F. Arrouy, E. Machler, T. Schneider, Ø. Fisher, and P. Martinoli, IBM Research Report RZ 2720, 07.03.95, 1995 (unpublished).
- ²⁵J. Olejniczak, A. J. Zaleski, and M. Cizek, Mod. Phys. Lett. B **8**, 185 (1994).
- ²⁶A. Porch, J. R. Cooper, D. N. Zheng, J. R. Waldram, A. M. Campbell, and P. A. Freeman, Physica C **214**, 350 (1993).
- ²⁷H. Parr, Phys. Rev. B **12**, 4886 (1975).
- ²⁸P. Imbert, G. Jehanno, C. Garciu, J. A. Hodges, and M. Bahout-Mouallem, Physica C **190**, 316 (1992).
- ²⁹J.-J. Chang and D. J. Scalapino, Phys. Rev. B **40**, 4299 (1989).
- ³⁰J. M. Tarascon, L. H. Greene, B. G. Bagley, W. R. McKinnon, P. Barboux, and G. W. Hull, in *Novel Superconductivity*, edited by S. A. Wolf and V. Z. Kresin (Plenum, New York, 1987), p. 705.
- ³¹H. Fujishita and M. Sato, Solid State Commun. **72**, 529 (1989).
- ³²K. A. Mirza, J. W. Loram, and J. R. Cooper, Physica C **282-287**, 1411 (1997).
- ³³D. A. Bonn, S. Kamal, K. Zhang, R. Liang, D. J. Baar, E. Klein, and W. N. Hardy, Phys. Rev. B **50**, 4051 (1994).
- ³⁴G. Xiao, M. Z. Cieplak, J. Q. Xiao, and C. L. Chien, Phys. Rev. B **42**, 8752 (1990).
- ³⁵B. Nachumi, A. Keren, K. Kojima, M. Larkin, G. M. Luke, J. Merrin, O. Tchernyshov, Y. J. Uemura, N. Ichikawa, M. Goto, and S. Uchida, Phys. Rev. Lett. **77**, 5421 (1996).
- ³⁶M. J. Sumner, J.-T. Kim, and T. R. Lemberger, Phys. Rev. B **47**, 12 248 (1993).
- ³⁷A. J. Zaleski and J. Klamut, Mol. Phys. Rep. **15/16**, 139 (1996).
- ³⁸A. J. Leggett, Physica B (Amsterdam) **199-200**, 291 (1994).
- ³⁹T. Xiang and J. M. Wheatley, Phys. Rev. Lett. **77**, 4632 (1996).
- ⁴⁰R. J. Radtke, V. N. Kostur, and K. Levin, Phys. Rev. B **53**, R522 (1996).
- ⁴¹S. V. Stolbov, J. Phys.: Condens. Matter **9**, 4691 (1997).